Terahertz Dynamics of a Topologically Protected State: Quantum Hall Effect Plateaus near the Cyclotron Resonance of a Two-Dimensional Electron Gas

A. V. Stier, C. T. Ellis, J. Kwon, H. Xing, H. Zhang, D. Eason, G. Strasser, T. Morimoto, H. Aoki, H. Zeng, B. D. McCombe, and J. Cerne

Phys. Rev. Lett. **115**, 247401 — Published 8 December 2015

DOI: 10.1103/PhysRevLett.115.247401

Terahertz dynamics of a topologically protected state: quantum Hall effect plateaus near cyclotron resonance in a two-dimensional electron gas

A.V. Stier[1], C.T. Ellis[1], , J. Kwon[1], H. Xing[1], H. Zhang[1] , D. Eason[1], G. Strasser[1],

T. Morimoto[2], H. Aoki[2], H. Zeng[1], B.D. McCombe[1] and J. Cerne[1]

[1]Department of Physics, University at Buffalo, The State University of New York, Buffalo, NY 14260, USA

[2]Department of Physics, University of Tokyo, Hongo, Tokyo 113-0033, Japan

We measure the Hall conductivity of a two-dimensional electron gas formed at a GaAs/AlGaAs heterojunction in the terahertz regime close to the cyclotron resonance frequency using highly sensitive Faraday rotation measurements. The sample is electrically gated, allowing the electron density to be changed continuously by more than a factor of three. We observe clear plateau- and step-like features in the Faraday rotation angle vs. electron density and magnetic field (Landau-level filling factor) even at fields/frequencies very close to cyclotron resonance absorption. These features are the high frequency manifestation of quantum Hall plateaus – a signature of topologically protected edge states. We observe both odd and even filling factor plateaus and explore the temperature dependence of these plateaus. Although dynamical scaling theory begins to break down in the frequency region of our measurements, we find good agreement with theory.

The dc quantum Hall effect (QHE) [1] has critically shaped our understanding of the physics of two-dimensional systems. This remarkable effect is the first example of a topologically protected state [2, 3]; the transverse Hall conductivity σ_{xy} is quantized by the suppression of backscattering in the quantum Hall edge channels. In spite of great progress in understanding the physics of the QHE, one particularly important question remains unanswered: How does the static Hall conductivity evolve into the dynamical (optical) Hall conductivity, $\sigma_{xy}(\omega)$? This has been partially addressed by experimental [4-11] and theoretical [12, 13] investigations. According to the localization picture, the QHE emerges from the coexistence of localized and delocalized states in disorder-broadened Landau levels (LL)[14]. The QHE plateau-to-plateau transitions take place over an energy interval *W* each time the Fermi energy passes from one localized region of the density of states (DOS) of a particular LL to another via delocalized states near the peak in the DOS [14]. When a critical energy E_c, which is located at the center of each disorder-broadened LL is approached, the localization length ξ diverges as a power law, $\xi(E) \sim |E - E_c|^{-\gamma}$. At zero frequency [2], the distinction between localized and delocalized states is clear; other than the topologically protected edge states, only states with localization length ξ larger than the sample size *L* can carry a dc current. For high frequency driving electric fields, the distinction is less clear, as both localized and delocalized states can contribute to the conductivity, with the localized states oscillating about their localization centers. When the amplitude of the oscillations of delocalized states becomes smaller than the dc ξ, localized and delocalized states become indistinguishable, and the signature of the QHE, the plateaus, disappears. Finite frequency ω and temperature T effectively shrink the sample size *W* (see Supplemental information). In this case, *W* is given by $W \sim T^{\kappa}$ and $W \sim \omega^{\kappa}$, where $\kappa = 1/z\,\gamma$

and therefore the components of the conductivity tensor exhibit a scaling behavior. Non-interacting electron systems [15, 16] as well as systems with short range interactions [17] are governed by a dynamical exponent $z = 2$; long-range interactions change the exponent to $z = 1$ [18]. Studies of the GHz longitudinal conductivity $\sigma_{xx}(\omega)$ reveal a scaling behavior with a critical exponent of $\kappa = 0.5 \pm 0.1$, yielding a dynamical exponent of $z = 0.9 \pm 0.1$ [4, 6]. This scaling picture is only valid in the low frequency region ($\omega << \omega_c$), and thus does not necessarily address the situation of the dynamical response close to cyclotron resonance (CR). Recently, Morimoto et al. have provided theoretical evidence that the step-like structure of the static Hall conductivity should survive even in the THz regime (1 THz = 10^{12} Hz, 4.22 meV, 33 cm^{-1}), despite the dynamical response being dominated by strong absorptive optical transitions between adjacent LLs (long red arrow in Fig. 1a) rather than weak intra-LL transitions (short blue arrow in Fig. 1a) [12]. Experimental work to test these predictions has been limited. Microwave measurements at magnetic fields where the radiation frequency (ω) is far below the cyclotron resonance frequency (ω_c), $\frac{\omega}{\omega_c} \ll 1$, have shown plateaus in $\sigma_{xy}(\omega)$ up to 33 GHz [4, 19], and a universal scaling in $\sigma_{xx}(\omega)$ up to 55 GHz [5, 6]. More recently, time domain THz spectroscopy was used [7] to measure $\sigma_{xy}(\omega)$ on an ungated GaAs/AlGaAs heterojunction, focusing on the region $\approx 0.2 - 0.6\,\omega_c$, which corresponds to a distance of 45 – 15 line widths away from CR, and shows an inflection point in $\sigma_{xy}(\omega)$ near filling factor 2. This inflection point was interpreted as a QHE plateau. Clear plateau-like behavior associated with the QHE near CR has yet to be observed and explored in spite of literally hundreds of publications on CR in GaAs 2-dimensional electron gases (2DEGs) since 1985 [20]. Recent results on the THz QHE [9] and infrared magneto-polarimetry at CR [9, 21, 22] in graphene further motivate our work.

We use a highly sensitive polarization-modulation technique to measure the Faraday angle of a 2DEG at the interface of a GaAs/AlGaAs heterostructure in the THz regime close to CR ($\frac{\omega}{\omega_c} \cong 1$)[23]. In the thin-film limit, the Faraday angle θ_F (the rotation of the plane of polarization of the electric field of the transmitted light) is directly proportional to the optical Hall conductivity through $\theta_F(\omega) + i\eta(\omega) \simeq \frac{1}{(1+n_s)c\epsilon_0}\sigma_{xy}(\omega)$ [7, 24, 25]. The line shape of the optical Hall conductivity around CR is given by the Drude expression, $\sigma_{xy}(\omega) = \frac{n\,e^2}{m_{eff}}\frac{\omega_c}{(i\omega+i/\tau)^2-\omega_c^2}$. In this region of strong CR absorption and dispersion we observe multiple clear and robust plateau- and step-like features in the Faraday rotation angle vs. electron density and B. These features appear near the expected regions of density and B that correspond to QHE plateaus at integer filling factors.

The system studied is a 2DEG formed at the interface of a GaAs/AlGaAs heterojunction ($n_{2\mathrm{D}}(V_g = 0) = 5.7 \times 10^{11}\mathrm{cm}^{-2}, \mu = 1.7 \times 10^5\mathrm{cm}^2/\mathrm{Vs}$ at $T = 77\mathrm{K}$). For these parameters, there is small density (~3%) of electrons in the first excited subband even at $V_g = 0$. At higher positive V_g, both subbands need to be taken into account (see Section 2 of the Supplemental Material). We use monochromatic emission lines from an optically pumped molecular gas laser and a polarization modulation technique [23, 24] (see Section 4 of Supplemental Material) to probe the Faraday angle, at two frequencies, 2.52 and 3.14 THz with a sensitivity better than 0.1^{o}. The high signal-to-noise ratio of these measurements allows us to investigate the scaling of the σ_{xy} plateaus with both frequency and temperature, and to compare it with theory [6, 12, 13].

Figure 1 summarizes our key results. The Faraday angle θ_F measured at 2.52 THz and T=1.6 K is shown in Fig. 1(b) as a function of B for a series of constant gate voltage (V_g). Two resonances are observed: a strong resonance feature that is consistent with predictions from the Drude model for CR in a 2DEG and a smaller feature near 6.2 T, which we associate with residual bulk carriers in the sample substrate. The inflection point of the large dispersive resonance feature marks the position of CR. The shift in position of the resonance feature to higher B as V_g and carrier density increase is consistent with an increase in the effective mass due to band non-parabolicity [26] (see inset Fig. 1(b)). We determine the 2D electron density n_{2D} as a function of V_g using dc Hall measurements on samples in the van der Pauw geometry. The measured n_{2D} agrees well with a simple capacitor model using the measured sample parameters. This allows us to translate our data into the parameter space $\left(\frac{\omega}{\omega_c}, \nu\right)$, where the cyclotron frequency $\omega_c = \frac{e\,B}{m_{\text{eff}}}$ and filling factor $\nu = \frac{n_{2D}h}{e\,B}$. Figure 1(c) shows θ_F measured at a higher THz frequency, $\omega_{THz} = 3.14\ \text{THz}$, plotted vs. $\frac{\omega}{\omega_c}$ and ν. The black arrows in Fig. 1 (b)-(d) mark the positions of integer filling factors. The ν=4 feature is very clear in Fig. 1b, where the positive peak height of several Faraday CR curves remains constant over a significant range of V_g. Note the plateau-like features at ν=3 and 4 as well as a clear step at ν=3.5 on the top ridgeline, and ν=6 on the bottom (minimum) ridgeline in the data in Fig. 1c).We attribute these features to QHE plateaus that we observe in the THz Faraday rotation, which are described in greater detail in Figs. 2-3 and the Supplemental Material. Note that both even and odd filling factor features are observed in the Faraday measurements. To compare our measured results with numerical calculations, we adopt the equation of motion (EOM) method [27], where

optical conductivities are described through EOM of the current density and disorder effects are treated as a phenomenological broadening for LLs. Theoretical calculations for a LL broadening $\frac{\Gamma}{\hbar\omega_c} = 0.03$ are shown in Fig. 1(d) and are in reasonable qualitative and quantitative agreement with the measurements. Specifically, simulation and experiment agree in the magnitude of θ_F and reproduce well the filling factor dependence at a particular $\frac{\omega}{\omega_c}$ (see Fig. 2(a)) for even filling factors. The calculations assume that the Zeeman splitting is negligible and therefore each LL is spin-degenerate, containing both spin-up and spin-down electrons [28].

We have further investigated θ_F as a function of V_g at a series of constant *B* above CR ($\omega_c > \omega$), which corresponds to changing ν at constant *B*. Before we discuss the results in detail, we compare the THz data with dc measurements (see Fig. 2(a)). Similar to results from [6], we find that THz and dc results generally track each other (the curves are offset in Fig. 2(a) for clarity). The dc data in Fig. 2(a) are taken at a slightly higher temperature of 1.9 K and involve sweeping B at constant V_g. As a result, the higher ν plateaus in the dc data are taken at smaller B (resulting in smaller LL and spin-splittings) so the spin-split plateaus are weakened compared to the 1.6 K measurements that sweep V_g at a higher B. Although the $\nu = 3$ plateau is very clear in the dc data, higher odd filling factor plateaus at $\nu = 5$ and to a much lesser extent at $\nu = 7$ are still visible. One would not expect to see odd filling factor plateaus in bulk GaAs at the *T* and *B* used in our measurements due to the small bulk g-factor. However, in a GaAs/AlGaAs 2DEG the g-factor is significantly enhanced due to many-body exchange interaction [29, 30]. We estimate the enhanced g-factor to range between $6.6 - 5.9$ from the lowest ($5 \times 10^{11} cm^2$) to the highest carrier densities($\sim 10^{12} cm^2$), respectively. This results in

a spin gap of approximately 2.5 meV (30 K) at 7 T. At 1.6 K and 7 T, the spin-splitting and the LL splitting of 11 meV (130 K) will both produce well-resolved plateaus, and we expect to see clearly spin-split LLs and thus plateaus at both even and odd filling factors. This is seen in the THz θ_F data in Fig. 2(a), especially for data that are recorded far away from CR. In THz θ_F data we see clear plateaus at $\nu = 4$ and 7 , as well as weaker features at $\nu = 3, 5, 6$ and 8. Figure 2(b) shows the THz θ_F vs. V_g at several fixed B. The QHE plateaus ride on the overall broad cyclotron resonance dispersion feature. Most notable is the evolution of the $\nu = 7$ plateau, which is washed out close to CR (6.49 T) and evolves into a distinct and broad plateau for increasing B above CR. Very close to CR at 6.46T, electron heating through the strong resonant absorption of THz radiation is likely responsible for the disappearance of the plateaus. Note also how the V_g positions for the $\nu = 4$ and 7 plateaus shift with B. This is expected since the carrier density at which these plateaus occur grows with increasing B. Figure 2(c) shows the THz θ_F as a function of ν at various fixed B. We observe a pronounced plateau-step feature for ν = 4 for all B fields. The overall magnitude of this feature diminishes for decreasing $\frac{\omega}{\omega_c}$, because the Drude background upon which it rides decreases. The Faraday signal is larger close to CR, which improves the signal-to-noise and therefore our ability to detect THz QHE plateaus. The plateau for $\nu = 5$ is barely visible as a slight inflection in the $\theta_F(\omega)$ vs. ν data. In contrast the next higher filling factor plateau ν = 6 is discernible very close to CR, but it then smears out and becomes comparable to the ν = 5 plateau at higher B. Note that the vertical spacing between plateaus (or where the Faraday data cross integer filling factor values) is not uniform. Since the Hall conductance is proportional to the Faraday angle, non-uniform spacing in θ_F implies that the THz Hall conductance is not quantized, which is one of the main predictions by Ref. [12].

Although B and ω are fixed during the V_g-sweeps, ω_c decreases slightly with increasing V_g due to the increase in effective mass with carrier density. As a result, $\frac{\omega}{\omega_c}$ approaches unity despite B and ω being constant, and CR absorption becomes stronger as V_g and ν increase. This is most clearly seen in the V_g scans at lower B in Fig. 2(c), where the θ_F background drops at higher ν, following the classical Faraday rotation dispersive line shape at CR.

Several plateaus are weak or missing under certain conditions. We attribute some of this behavior to the overlap of LLs in the first excited subband with LLs in the ground subband. A qualitative explanation of this effect is provided in the Supplemental Material Section 2.

The observed THz plateau structures are sensitive to temperature as depicted in Fig. 3. The temperature dependence of the odd filling factor plateaus $\nu = 1$ and 3 for dc magneto-transport is consistent with the temperature dependence of the exchange enhanced g-factor. As shown in Figure 3 a), the odd plateaus quickly smear out as temperature increases from 2 K to 4 K, while the even plateau $\nu = 2$ remains nearly unchanged. We also clearly see even filling factor plateaus in dc measurements at 9 K. On the other hand, Figure 3 b.) shows that the THz $\nu = 4$ plateau at $\left(\frac{\omega}{\omega_c}\right) = 0.97$ strongly depends on temperature, disappearing by 5 K. The plateau width is plotted in the inset. We can describe the decrease of the plateau width using a power law with an exponent of $\kappa = 0.5 \pm 0.1$, which is consistent with temperature scaling behavior in the GHz regime [6] and points towards an electron-electron interaction mechanism for the temperature dependence of even plateaus in the THz regime. Note that the washing out of the THz plateau cannot be solely attributed to thermal effects since the energy splitting

responsible for the plateau is approximately 11 meV (130 K), which is significantly larger than $k_B T$ at 5 K.

In conclusion, we have observed clear step-like and plateau-like features close to even and odd integer filling factors in the THz $\sigma_{xy}(\omega)$. Results are analyzed with and compared to recent calculations. Unlike previous GHz and THz studies of $\sigma_{xy}(\omega)$, where the only allowed optical transitions correspond to *intra*-LL processes $(\omega \ll \omega_c)$, it is remarkable that in our measurements, the dc QHE effect is found to persist in a regime where the conductivity is dominated by strong *inter*-LL photon absorption $(\omega \sim \omega_c)$. It is interesting to observe that the polarization of THz photons close to inter-Landau level (cyclotron) absorption is sensitive to whether the Fermi energy lies in localized or delocalized levels, producing QHE plateaus. The temperature scaling of the THz plateau widths is consistent with electron-electron interaction processes.

This work was supported by NSF-DMR1006078 (CTE & JC), NSF-MWN1008138 (AVS & BDM), HA has been supported in part by a Grant-in-Aid for Scientific Research No. 23340112 from MEXT and TM by JSPS. We gratefully acknowledge M. Pakmehr and A. Mukherjee for preliminary dc magneto-transport measurements. We thank M. Grayson for critical advice on processing gates for the samples used in the final dc magnetotransport measurements. We also thank S. Ganapathy for helpful discussions on the QHE.

[1] K. v. Klitzing, G. Dorda, and M. Pepper, Physical Review Letters **45**, 494 (1980).
[2] J. E. Avron, D. Osadchy, and R. Seiler, Physics Today **56**, 38 (2003).
[3] D. J. Thouless *et al.*, Physical Review Letters **49**, 405 (1982).
[4] F. Kuchar *et al.*, Physical Review B **33**, 2965 (1986).
[5] L. W. Engel *et al.*, Physical Review Letters **71**, 2638 (1993).
[6] F. Hohls *et al.*, Physical Review Letters **89**, 276801 (2002).
[7] Y. Ikebe *et al.*, Physical Review Letters **104**, 256802 (2010).
[8] A. V. Stier *et al.*, AIP Conference Proceedings **1399**, 627 (2011).
[9] R. Shimano *et al.*, Nat Commun **4**, 1841 (2013).
[10] R. Shimano *et al.*, EPL (Europhysics Letters) **95**, 17002 (2011).
[11] G. S. Jenkins, D. C. Schmadel, and H. D. Drew, Review of Scientific Instruments **81**, 083903 (2010).
[12] T. Morimoto, Y. Hatsugai, and H. Aoki, Physical Review Letters **103**, 116803 (2009).
[13] T. Morimoto, Y. Avishai, and H. Aoki, Physical Review B **82**, 081404 (2010).
[14] H. Aoki, and T. Ando, Solid State Communications **38**, 1079 (1981).
[15] B. M. Gammel, and W. Brenig, Physical Review B **53**, R13279 (1996).
[16] J. T. Chalker, Journal of Physics C: Solid State Physics **21**, L119 (1988).
[17] D.-H. Lee, and Z. Wang, Physical Review Letters **76**, 4014 (1996).
[18] D. G. Polyakov, and B. I. Shklovskii, Physical Review B **48**, 11167 (1993).
[19] V. A. Volkov *et al.*, Pis'ma Zh. Eksp. Theor. Fiz. (JETP Letters) **43**, 255 (1986).
[20] Based on a Web of Science topic search using "GaAs cyclotron resonance" which returned 1,211 papers (12/30/2011).
[21] C. T. Ellis *et al.*, in Infrared, Millimeter, and Terahertz Waves (IRMMW-THz), 2012 37th International Conference on2012), pp. 1.
[22] C. T. Ellis *et al.*, Sci. Rep. **3** (2013).
[23] D. K. George *et al.*, J. Opt. Soc. Am. B **29**, 1406 (2012).
[24] M. Grayson *et al.*, Physical Review Letters **89**, 037003 (2002).
[25] Interestingly, Drude calculations show that at lower carrier densities such as in our GaAs/AlGaAs 2DEG, $\theta_F \propto \sigma_{xy}$, while in higher density metallic systems $\theta_F \approx \theta_H$ in the THz range, where $\theta_H = \sigma_{xy}/\sigma_{xx}$ is the Hall angle.
[26] T. Ando, J. Phys. Soc. Jpn. **51**, 3893 (1982).
[27] A. Ferreira *et al.*, Physical Review B **84**, 235410 (2011).
[28] Note that in Figs. 1c and 1d, θ_F decreases as $\frac{\omega}{\omega_c}$ approaches zero. By converting our dc σ_{xx} and σ_{xy} measurements into a dc (frequency approaching zero) θ_F we can compare the dc and THz values of θ_F. Our measured dc θ_F is

about 0.1 degree, which is more than two orders of magnitude smaller than the THz θ_F that we measure near the cyclotron frequency. This is consistent with a simple Drude model.

[29] D. R. Leadley *et al.*, Physical Review B **58**, 13036 (1998).
[30] I. L. Aleiner, and L. I. Glazman, Physical Review B **52**, 11296 (1995).

Figure captions

Fig.1: a) Cartoon of Drude-like intra-band transitions (blue arrow) and circularly active CR inter-band transitions (yellow arrow) between adjacent LL. b) Faraday rotation for $\omega_{THz} = 2.52\ \mathrm{THz}$ versus magnetic field *B* at various, fixed gate voltages V_g. The large background is due to CR. Inset shows shift of effective electron mass as function of V_g. c) The measured Faraday rotation for $\omega_{THz} = 3.14\ \mathrm{THz}$ versus *B* at various fixed V_g translated into the parameter space $\left(\frac{\omega}{\omega_c}, \nu\right)$. Integer filling factor positions are labeled with black arrows. d) Theoretical predictions of $\theta_F(\frac{\omega}{\omega_c}, \nu)$ showing plateau structure at similar filling factors. The calculation neglects spin splitting (which we show occurs for our system) and therefore only shows spin-degenerate plateaus at even Landau level filling factors.

Fig. 2: a) THz Faraday measurements, dc Hall conductance measurements, and numerical THz Faraday simulations plotted as functions of filling factor ν. dc Hall conductance (blue solid) along with THz Faraday rotation vs. filling factor for B=6.62T ($\omega_{THz} = 2.52\ \mathrm{THz}$, purple crosses). Weak $\nu = 3,\ 5, 6\ \mathrm{and}\ 8$ as well as strong $\nu = 4$ and $\nu = 7$ plateau features are seen. Curves are offset for clarity. Numerical simulation for $\frac{\Gamma}{\hbar\omega_c} = 0.03$ are shown by the grey solid)line. Note that the numerical simulations explicitly assume spin degenerate Landaus levels, and hence only show even filling factor plateaus. b) and c) Faraday rotation vs. V_g and filling factor ν for various fixed magnetic fields, increasing in increments of ~0.1 T from 6.46 T to 7.28 T.

Fig.3: a) DC Hall conductance vs. filling factor for *T*=2 K (blue solid) and *T*=4 K (red dashed) at a density of $n_{2D} = 5.5 \times 10^{11} cm^{-2}$. b) THz Faraday rotation as a function of filling factor at $\frac{\omega}{\omega_c} = 0.97$ and at *T* = 1.8 K (black solid line), *T* = 2.2 K (red dashed) and *T* = 5.0 K (green dotted). The inset shows the plateau width as a function of temperature. Lines are calculated after [6] with exponent $\kappa = 0.5$ (solid), $\kappa = 0.6$ (dashed) and $\kappa = 0.4$ (dotted).

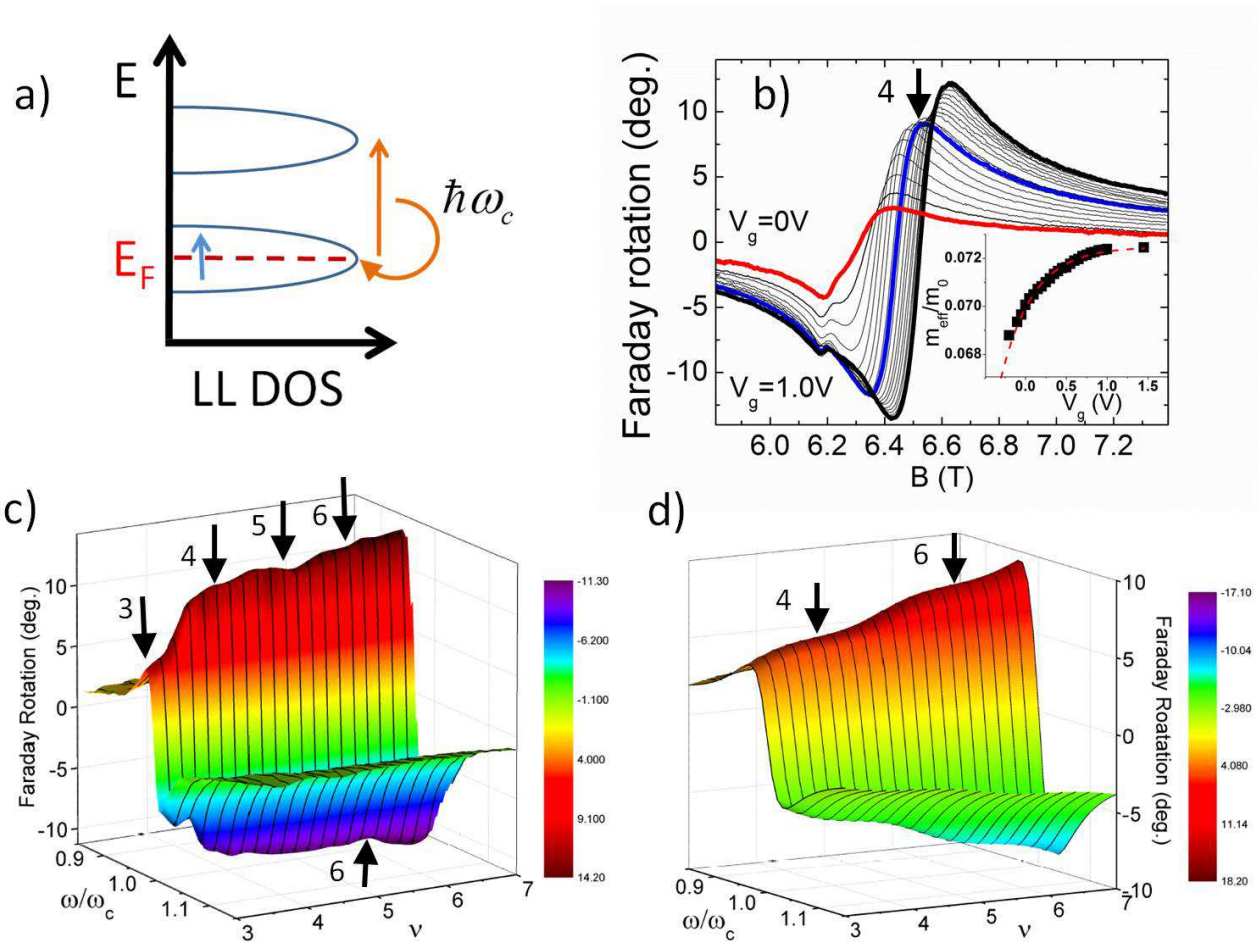

Figure 1 LN12594 16OCT2015

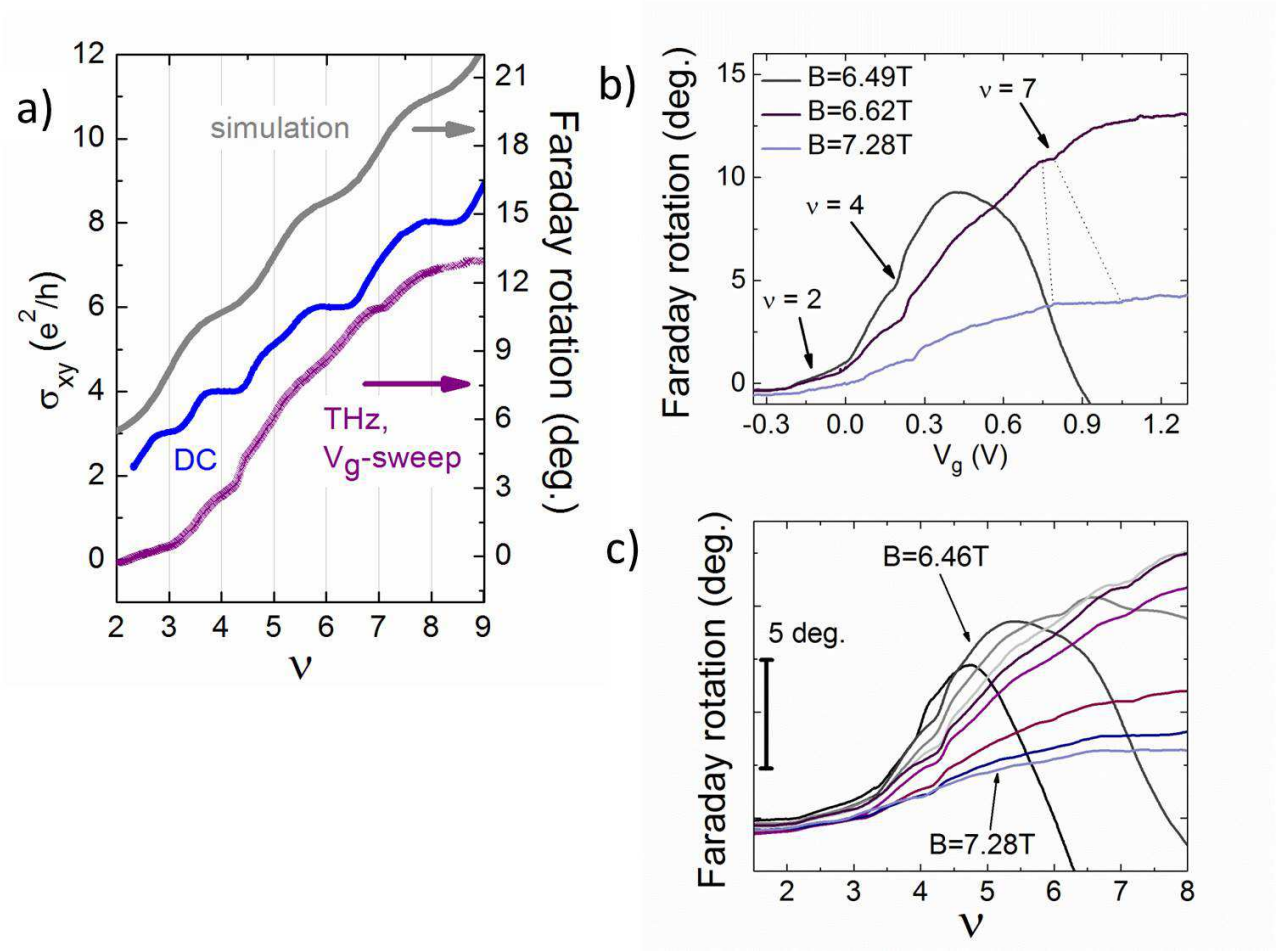

Figure 2 LN12594 16OCT2015

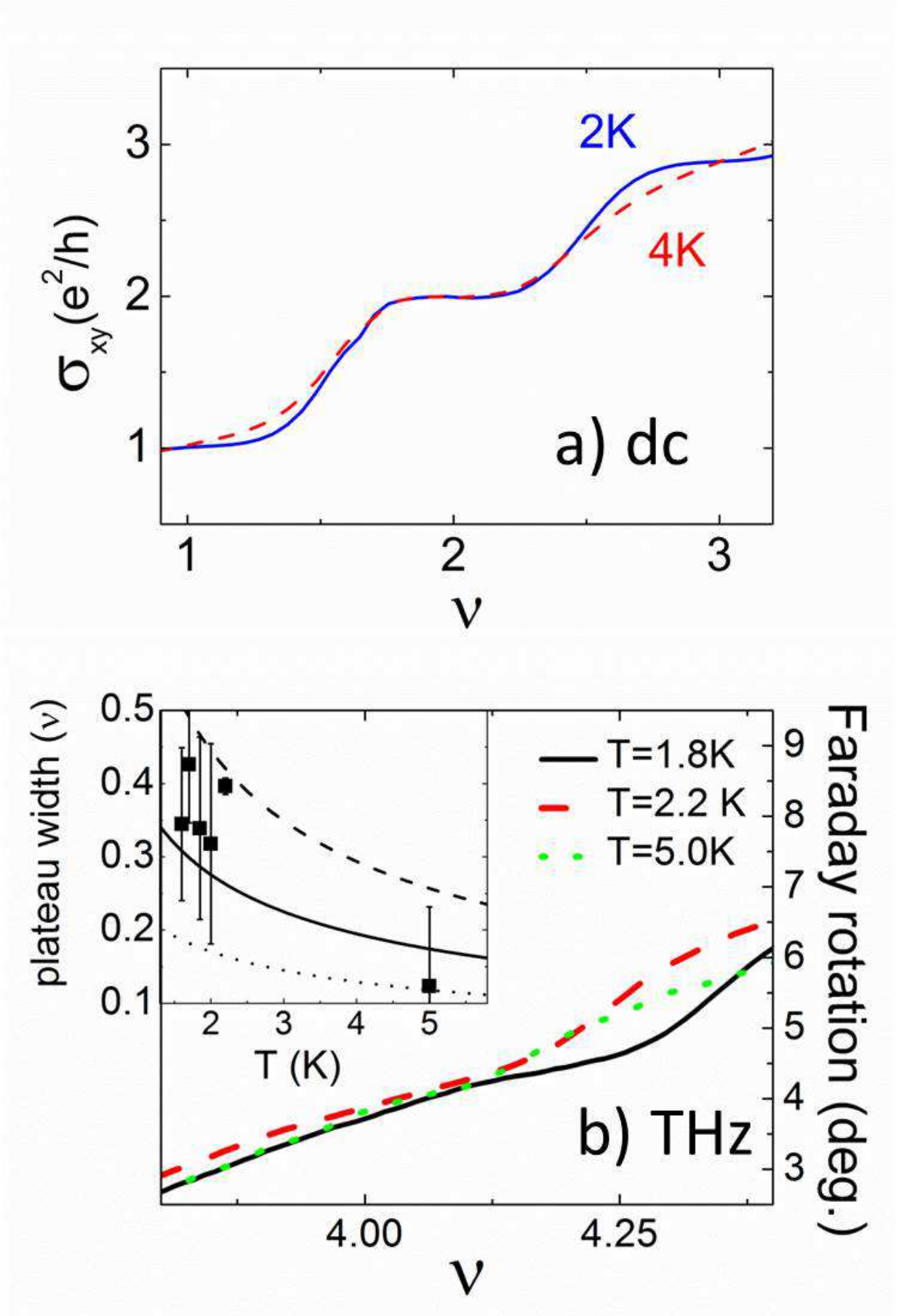

Figure 3 LN12594 16OCT2015